

Synthesis and Characterization of ZnO/Ag-Doped ZnO Core–Shell Nanowires

Xuan Fang¹, X. Y. Wang², Jilong Tang^{1,*}, Fang Fang^{1,3,*}, Shanshan Lu¹,
Xujie Wang¹, Shuangpeng Wang⁴, Haifeng Zhao⁴, Dan Fang¹, Jinhua Li¹,
Xueying Chu¹, Fei Wang¹, Xiaohua Wang¹, and Zhipeng Wei¹

¹State Key Laboratory of High Power Semiconductor Laser, School of Science, Changchun University of Science and Technology, Changchun 130022, People's Republic of China

²Department of Civil Engineering, Northeast Dianli University, Jilin 132012, China

³Nanchang University, Jiangxi Province, Nanchang 330047, People's Republic of China

⁴Changchun Institute of Optics, Fine Mechanics and Physics,
Chinese Academy of Science, Changchun, 130033, People's Republic of China

In this work, the ZnO/Ag-doped ZnO core–shell nanowires were obtained through a facile three-step method, including the hydrothermal process for ZnO nanowires growth, DC sputtering for silver particles deposition on ZnO nanowires and atom layer deposition for ZnO shell layer deposition. The *p*-type ZnO shell layer was achieved by annealing treatment under oxygen-rich condition. Compared with ZnO and ZnO/Ag/ZnO samples, (002) diffraction peak position of ZnO/Ag-doped ZnO core–shell nanowires shifted to small angle side, which indicated that Ag diffused into ZnO lattice as shell layer. Meanwhile, low-temperature photoluminescence (PL) was used to investigate the *p*-type emission behavior, which can be observed by exciton bound to a neutral acceptor (A^0X) at 3.354 eV and the recombination of free electron to the acceptor transition (FA) at 3.315 eV in such the Ag-doped ZnO shell layer. In addition, the calculated acceptor binding energy was 124 meV.

Keywords: Ag-Doped ZnO, *p* Type Doping, Core–Shell Nanowires, Atom Layer Deposition.

1. INTRODUCTION

As a wide band gap semiconductor material, ZnO can be used to fabricate ultraviolet light-emitting diodes, laser and biosensor. Generally, the defects and impurities are the key factors to dominate semiconductors' optoelectronic behaviors.^{1–4} For better expanding the applications of ZnO,^{5–9} metal ion doping is an active and leading method currently. Considerable works have been reported on the doping of ZnO with several dopants to tailor its electrical and optical properties by different methods.^{4, 10, 11} Due to its own existence of zinc vacancy and O interstice, Pure ZnO materials show a natural *n*-type characteristic. However, in order to obtain *p*-type ZnO, the I group elements substitute for zinc site from ZnO lattice to form the acceptor level in ZnO. Ag-doping in ZnO is able to change the optoelectronic properties of ZnO thin films and nanostructures, while early researches showed that Ag incorporation in ZnO reduced the donor density.^{11, 12} Because of the calculated formation energy was much lower for Ag_{Zn}

substitutional site than interstitial ones, which made Ag an effective acceptor in ZnO.¹³ And many research works confirm the *p*-type conductivity is stable in Ag-doped ZnO samples.

For practical application, compared with ZnO heterojunction, ZnO homojunction has lower mismatch degree of the interface to avoid low quantum efficiency from quantum traps or recombination centers, especially for ZnO based nanostructures devices. And in this paper, a ZnO core–shell nanowires with Ag-doped ZnO layer were obtained, which were formed by direct current sputtering and atomic layer deposition (ALD).¹⁴ The structure and optical properties of the samples were investigated in details. From the low-temperature and temperature dependent PL spectra, the emission related to the Ag acceptor was detected, which indicate the type conversion from *n*-type to *p*-type in such Ag-doped ZnO shell structure.

2. EXPERIMENTAL DETAILS

Figure 1 is the schematic of the formation process of ZnO/Ag-doped ZnO core–shell nanowires. First, ZnO

*Authors to whom correspondence should be addressed.

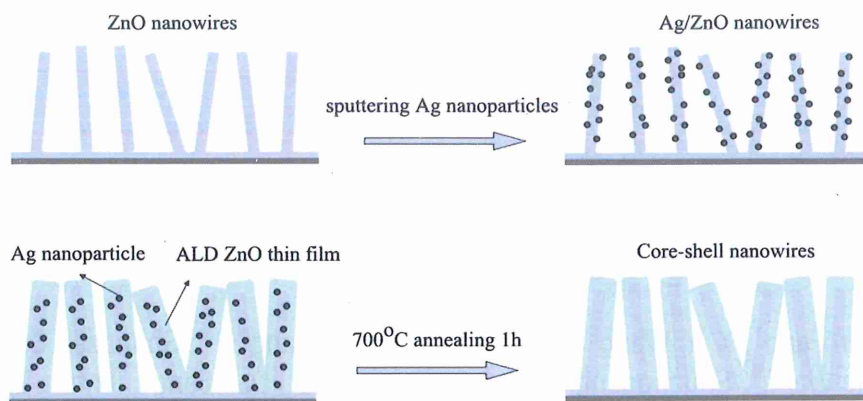


Fig. 1. The schematic representation of the formation process of ZnO/Ag-doped ZnO core-shell nanowires.

nanowires were synthesized on quartz substrate coated by ZnO seed films using hydrothermal method, 0.01 mol/L $\text{Zn}(\text{CH}_3\text{COO})_2 \cdot 2\text{H}_2\text{O}$ and 0.01 mol/L hexamethylenetetramine (HMT) were dissolved in 100 ml deionized water well and removed the high-pressure reaction kettle with 15 ml aqueous solution into the drying oven at 90 °C for reacting 6 h. After the reaction, the autoclave was taken out of the oven and cooled to room temperature. Later the sample was washed thoroughly with by deionized water and dried at 60 °C for 1 h. Then, Ag nanoparticles were deposited on ZnO nanowires under 6 mA discharge current for 60 s by DC sputtering. The shell layer ZnO were grown using LabNanoTM 9100^{2nd} ALD system from Ensure Nanotech (Beijing). Water and Diethyl zinc (DEZn , $\text{Zn}(\text{C}_2\text{H}_5)_2$) were used as precursors and were kept at room temperature. High purity nitrogen (N_2) was used as the purging gas. Water and DEZn were introduced into the growth chamber separately. N_2 purge was introduced after precursors pulse to remove the residues and byproducts. The pulse time of water and DEZn was 20 ms and the purging time was 8 s. The growth temperature was 170 °C. The cycles of growth were 500 cycles. At last, the samples were annealed in tube furnace under O-rich condition for 1 h, the temperature was 700 °C.

All samples were investigated by scanning electron microscopy (SEM, JEOL-6010LA). And the crystal structure of the ZnO nanowires and ZnO/Ag-doped ZnO core-shell nanowires were characterized by X-ray Diffraction (Bruker AXS D8 DAVINCI) with Cu-K α radiation ($\lambda = 1.5406 \text{ \AA}$). Photoluminescence (PL) measurements were performed using a He-Cd laser line of 325 nm as the excitation source.

3. RESULTS AND DISCUSSION

The SEM images of ZnO nanowires are shown in Figure 2(a). We observe that ZnO nanowires have a smooth hexagonal shape surface, the nanowires have a typical diameter of about 100 nm and a length of a few micrometers. The SEM image of ZnO/Ag/ZnO nanowires and annealed samples are shown in Figures 2(b) and (c).

Compared with ZnO nanowires, the surface of the two samples become roughness (from the inset of Figs. 2(b) and (c)). In addition, the diameter of the two samples are about 500 nm. And after annealing treatment, the core-shell structure could be obtained, which can be seen in the inset of Figure 2(c). In Figure 2(d), the EDX spectrum presents the existence of Ag element at the ZnO/Ag-doped ZnO core-shell nanowires.

The changes of crystal phase structure of the samples were investigated by X-ray diffraction. In Figure 3, based on standard PDF card (No.36-1451), For ZnO nanowires, the (100), (002) and (101) diffractive peaks correspond at 34.31°, 34.40°, 34.52° could be observed which were indexed to ZnO wurtzite structure. For ZnO/Ag/ZnO nanowires, we merely observe Ag_2O (111) diffraction peak at 32.853° (PDF No.75-1532) while no other impurity phases peak, which meant the Ag particles were existed by Ag_2O phase. For core-shell nanowires, this samples exhibited the better *c*-axis orientation and narrower full width at half maxima (FWHM). And compared with ZnO and ZnO/Ag samples, a slight shift of (002) diffraction peak can be observed. The magnification of (002) peak of three samples are shown in the inset of Figure 3. The (002) peak of ZnO/Ag-doped core-shell samples moved 0.07°, which confirms Ag successfully diffused into the ZnO crystal lattice.

Figure 4 indicated the room temperature PL spectra of ZnO, ZnO/Ag, ZnO/Ag-doped ZnO core-shell sample, respectively. In ZnO sample, the near the band-edge (NBE) emission peak at 379 nm and deep level defects emission peak at 450 ~ 650 nm can be detected.¹⁵⁻¹⁹ Compared with ZnO sample, ZnO/Ag has a stronger NBE emission. This phenomenon is caused by surface plasmon enhancement of Ag particles.²⁰ And NBE emission of ZnO/Ag-doped ZnO core-shell samples is also enhancement.¹⁴ Meanwhile, due to the annealing treatment under O-rich condition, the green light excitation from deep level defects emission is attenuated. In Kim et al. report,²¹ annealed ZnO:Ag thin film have a drastic enhancement at NBE emission while a slight decrease in the deep level emission, which support

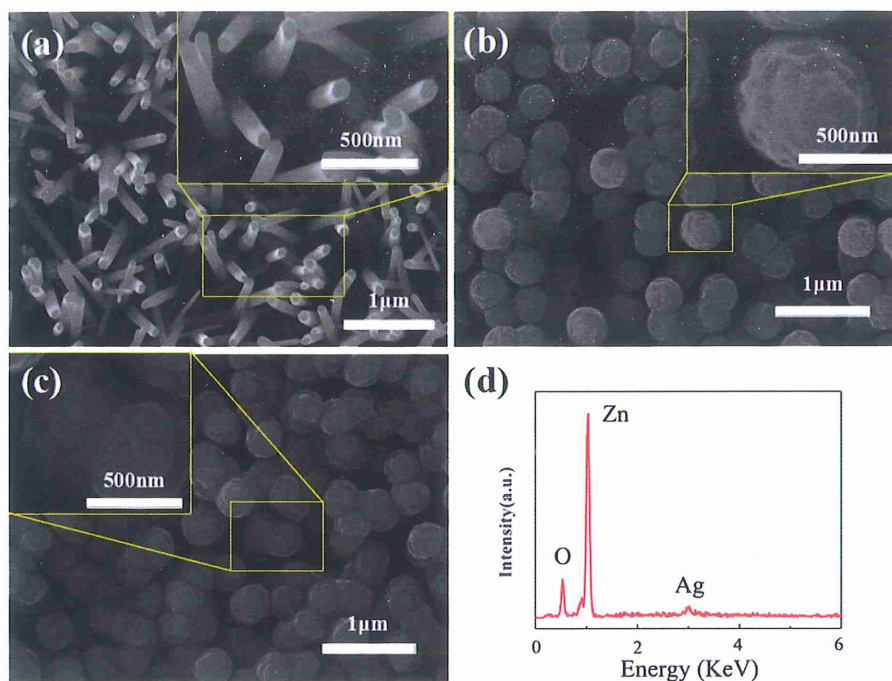


Fig. 2. The SEM images of (a) ZnO nanowires, (b) as-grown ZnO/Ag/ZnO sample; (c) ZnO/Ag-doped ZnO core-shell sample; (d) EDX spectrum of ZnO/Ag-doped ZnO core-shell nanowires sample.

that the existence of holes and electrons easily arrived at interface between Ag_2O and ZnO film. Ag particles was not placed at the interstitial sites or as defects in ZnO while after annealing process, which were the main reasons of NBE emission enhancement and the largely suppression of deep level emission.

Low-temperature PL spectroscopy is a useful tool for characterizing acceptor/donor impurities. Low-temperature PL spectra of ZnO and ZnO/Ag-doped ZnO core-shell nanowires sample can make us to understand the optical performances deeply. Figure 5 shows the Low-temperature

PL spectra of ZnO (Fig. 5(a)) and annealed core-shell ZnO nanowires (Fig. 5(b)) at 85 K. In Figure 5(a), For ZnO sample, we can find a emission peak at 3.364 eV. The emission peak of 3.364 eV is assigned to the radiative recombination of neutral donor-bound exciton (D^0X).¹² In Figure 5(b), annealed ZnO/Ag-doped ZnO core-shell nanowires sample, the low temperature PL spectrum shows that emission peak at 3.243 eV, 3.315 eV, 3.354 eV, 3.367 eV, respectively. The peak at 3.367 eV assigned to D^0X . The peak at 3.354 eV comes from the neutral acceptor-bound exciton (A^0X) emission in ZnO.²² According to the previous reports of doped ZnO nanowires,^{12, 22, 23} we know the origination of 3.315 eV and 3.243 eV are

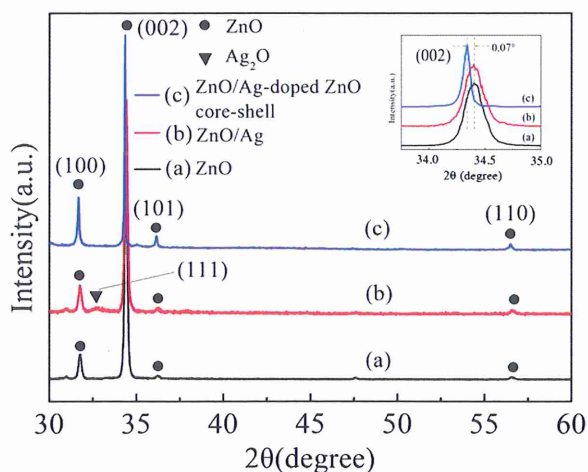


Fig. 3. XRD patterns of (a) ZnO, (b) ZnO/Ag, (c) ZnO/Ag-doped ZnO core-shell, respectively. Inset shows the (002) diffraction peak of (a) ZnO, (b) ZnO/Ag, (c) ZnO/Ag-doped ZnO core-shell, respectively.

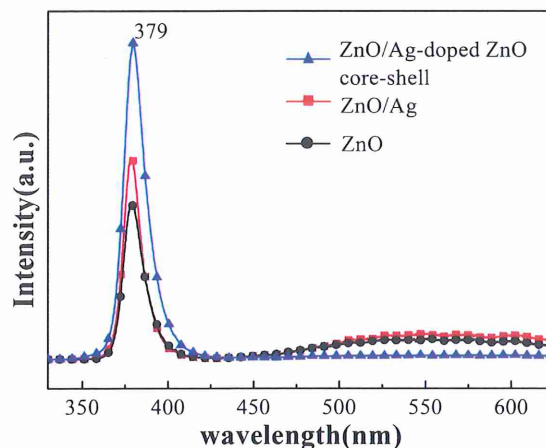


Fig. 4. Room temperature PL spectra of ZnO, ZnO/Ag, ZnO/Ag-doped ZnO core-shell, respectively.

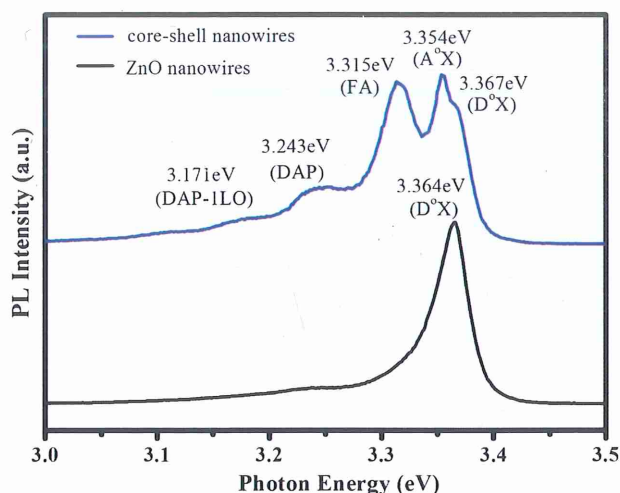


Fig. 5. Low-temperature PL spectra of (a) ZnO and (b) ZnO/Ag-doped ZnO core-shell at 85 K.

related to acceptors in ZnO. The emission at 3.315 eV is assigned to the recombination of free electron to the acceptor transition (FA) and the emission at 3.243 eV is assigned to the recombination of the donor-acceptor pair (DAP).¹² We observed the new peak of 3.354 eV, 3.315 eV and 3.243 eV, which were related to acceptor-bound exciton peaks in annealed ZnO shell layer.

According to the previous report,^{24–26} FA is often observed at *p*-type doped ZnO sample. To further understand the origination of the emissions, temperature-dependent PL spectra and temperature fitting curve of FA emission peak of annealed ZnO/Ag-doped ZnO core-shell nanostructures were investigated (shown in Fig. 6). In Figure 6(a), the temperature-dependent PL spectra of FA emission 3.315 eV (85 K). With the temperature increasing, FA emission transition energy indicated a continuous red-shift. The FA binding energy peak is fit using the following expression (1).

$$E_{FA}(T) = E_g(T) - E_A + K_B T/2 \quad (1)$$

E_A and E_{FA} is the binding energy of the acceptor involved and free electron to acceptor energy, respectively. $E_g(T)$ is the temperature-dependent band gap energy, K_B is Boltzmann's constant, and T is temperature. $E_g(T)$ corresponding to expression of Varshni's formula (2)

$$E_g(T) = E_g(0) - \alpha T^2/(T + \beta) \quad (2)$$

$E_g(0)$ is the band gap energy at 0 K and α and β were determined to be 1.0×10^{-3} eV/K and 925 K. The acceptor binding energy of E_A is approximately 124 meV. In Figure 6(b), the FA emission sampling points of annealed sample is coincide with theoretical fitting peak curve approximately. The above results are agreed with previous reports.²⁴ This is another proof that Ag was introduced into the ZnO crystal lattice.

In a word, the new peaks of ZnO/Ag-doped ZnO core-shell nanowires are related to accepters.

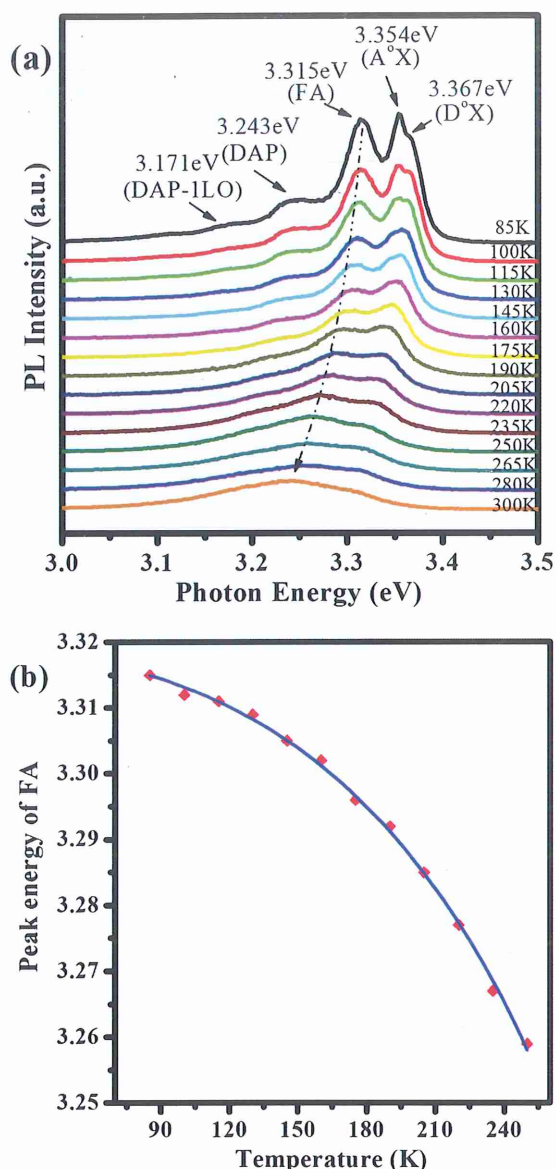


Fig. 6. (a) Temperature-dependent PL spectra of annealed ZnO/Ag-doped ZnO core-shell nanowires; (b) FA emission peak curve fitting with temperature.

The low-temperature PL spectra show a main NBE emission at 3.354 eV, which is attributed to A^0X . The peaks located at 3.315 eV and 3.243 eV are attributed to free exciton to the acceptor transition and DAP transition, respectively. With increasing temperature, FA emission peak is continuing red-shift and DAP transition is vanishing in high temperature. The temperature-dependent PL spectrum of ZnO/Ag-doped ZnO core-shell nanowires prove that D^0X and FA emission are primarily composition of room-temperature UV emission.

4. CONCLUSIONS

In summary, ZnO/Ag-doped ZnO core-shell nanowires were synthesized, a series of characterization

measurements demonstrate that Ag ions have been diffused into ZnO lattice, and such ZnO/Ag-doped ZnO core–shell nanowires have a good crystalline quality. Through analyzing and comparing the crystal structure and optical properties, we found that the XRD peaks of ZnO/Ag-doped ZnO core–shell nanowires had a small-angle shift of 0.07° from 34.43° to 34.36° . Low-temperature PL measurement show the neutral acceptor related emission at 3.354 eV (A^0X) and 3.315 eV (FA). The calculated acceptor binding energy is 124 meV. The experiences obtained from this research will be a useful for subsequent study in the preparation of *p*-type ZnO and functional ZnO/metal nanocomposites, as well as a valuable reference for researchers of nanodevices engineering.^{27–30}

Acknowledgments: This work is supported by the National Natural Science Foundation of China (61076039, 61204065, 61205193, 61307045, 21103159), National Key Lab of High Power Semiconductor Lasers Foundation (No.9140C310101120C031115), Research Fund for the Doctoral Program of Higher Education of China (21022216110002, 20102216110001, 20112216120005), the Developing Project of Science and Technology of Jilin Province (20121816, 201201116), the Foundation of Department of Education of Jilin Province (2011JYT05, 2011JYT10, 2011JYT11). Thanks for the help of D. D. Wang, Y. S. Yan. for the SEM measurement, and D. J. Wang of Ensure Nanotech for the ALD experiment.

References and Notes

1. J. J. Lee, G. Z. Xing, J. B. Yi, T. Chen, M. Ionescu, and S. Li, *Appl. Phys. Lett.* 104, 012405 (2014).
2. D. D. Wang, G. Z. Xing, F. Yan, Y. S. Yan, and S. Li, *Appl. Phys. Lett.* 104, 022412 (2014).
3. G. Z. Xing, D. D. Wang, C.-J. Cheng, M. He, S. Li, and T. Wu, *Appl. Phys. Lett.* 103, 022402 (2013).
4. H. K. Liang, S. F. Yu, and H. Y. Yang, *Appl. Phys. Lett.* 96, 101116 (2010).
5. Y. Y. Lai, Y. P. Lan, and T. C. Lu, *Light: Science and Applications* 2, e76 (2013).
6. J. Yang, F. F. Luo, T. S. Kao, X. Li, G. W. Ho, J. H. Teng, X. G. Luo, and M. H. Hong, *Light: Science and Applications* 3, e185 (2014).
7. K. Ding and C. Z. Ning, *Light: Science and Applications* 1, e20 (2012).
8. Y. Z. Huang, Y. R. Fang, Z. L. Zhang, L. Zhu, and M. T. Sun, *Light: Science and Applications* 3, e199 (2014).
9. A. Lundskog, C. W. Hsu, K. F. Karlsson, S. Amloy, and D. Nilsson, *Light: Science and Applications* 3, e139 (2014).
10. G. Z. Xing, J. B. Yi, F. Yan, T. Wu, and S. Li, *Appl. Phys. Lett.* 104, 202411 (2014).
11. Z. P. Wei, B. Yao, Z. Z. Zhang, Y. M. Lu, D. Z. Shen, B. H. Li, X. H. Wang, J. Y. Zhang, D. X. Zhao, X. W. Fan, and Z. K. Tang, *Appl. Phys. Lett.* 89, 102104 (2006).
12. X. Fang, J. H. Li, D. X. Zhao, D. Z. Shen, B. H. Li, and X. H. Wang, *J. Phys. Chem. C* 113, 21208 (2009).
13. F. Fang, D. X. Zhao, X. Fang, J. H. Li, Z. P. Wei, S. Z. Wang, J. L. Wu, and X. H. Wang, *J. Mater. Chem.* 21, 14979 (2011).
14. X. Fang, S. L. Li, X. H. Wang, F. Fang, X. Y. Ch, Z. P. Wei, J. H. Li, X. Y. Chen, and F. Wang, *Appl. Surf. Sci.* 263, 14 (2012).
15. J. Q. Xu, G. H. Hou, B. P. Dong, Y. Y. Chang, Y. R. Wang, H. L. Yan, and B. H. Yu, *Nanosci. Nanotechnol. Lett.* 5, 1081 (2013).
16. J. Wu, J. Xia, J. Chen, W. Lei, B. P. Wang, Y. F. Zhang, and D. D. Engelsena, *Nanosci. Nanotechnol. Lett.* 6, 1005 (2014).
17. R. Deng, Y. F. Li, B. Yao, J. M. Qin, D. Y. Jiang, X. Fang, F. Fang, Z. P. Wei, and L. L. Gao, *Nanosci. Nanotechnol. Lett.* 6, 887 (2014).
18. X. Chen and Z. J. Liu, *Nanosci. Nanotechnol. Lett.* 7, 726 (2013).
19. C. X. Wu, M. Zhou, S. G. Zhang, and L. Cai, *Nanosci. Nanotechnol. Lett.* 5, 174 (2013).
20. L. Duan, B. X. Lin, W. Y. Zhang, S. Zhong, and Z. X. Fu, *Appl. Phys. Lett.* 88, 232110 (2006).
21. K. Kim, D. H. Lee, S. Y. Lee, G. E. Jang, and J. S. Kim, *Nanoscale Res. Lett.* 7, 273 (2012).
22. B. Q. Cao, M. Lorenz, A. Rahm, H. V. Wenckstern, C. Czekalla, J. Lenzner, G. Benndorf, and M. Grundmann, *Nanotechnology* 18, 455707 (2007).
23. X. Li, C. Y. Li, T. Kawaharamura, D. P. Wang, N. Nitta, M. Furuta, H. Furuta, and A. Hatta, *Nanosci. Nanotechnol. Lett.* 6, 174 (2014).
24. C. X. Shan, Z. Liu, and S. K. Hark, *Appl. Phys. Lett.* 92, 073103 (2008).
25. C. H. Zang, D. X. Zhao, Y. Tang, Z. Guo, J. Y. Zhang, D. Z. Shen, and Y. C. Liu, *Chem. Phys. Lett.* 452, 148 (2008).
26. M. Schirra, R. Schneider, A. Reiser, G. M. Prinz, M. Feneberg, J. Biskupek, U. Kaiser, C. E. Krill, K. Thonke, and R. Sauer, *Phys. Rev. B* 77, 125215 (2008).
27. V. A. Kulbachinskii, P. V. Gurin, and L. N. Oveshnikov, *Nanosci. Nanotechnol. Lett.* 4, 634 (2012).
28. S. C. Chen, T. Y. Kuo, W. C. Peng, S. L. Ou, and H. C. Lin, *Nanosci. Nanotechnol. Lett.* 8, 883 (2013).
29. Y. H. Su, Y. F. Ke, S. L. Cai, and Q. Y. Yao, *Light: Science and Applications* 1, e14 (2012).
30. D. Lepage, A. Jiménez, J. Beauvais, and J. J. Dubowski, *Light: Science and Applications* 1, e28 (2012).

Received: 19 July 2014. Revised/Accepted: 11 February 2015.